Mechanical Behavior of Reinforced Silty Sand: Focus on Application of Nano-Silica or Kaolin Coated Ceramic Fibers as a Reinforcement Material

Mehdi Eshaghzadeh
  Islamic Azad University Najafabad Branch

Meysam Bayat (✉ bayat.m@pci.iaun.ac.ir)
  Islamic Azad University Najafabad Branch   https://orcid.org/0000-0001-5525-5199

Rassoul Ajalloeian
  Isfahan University of Technology

Sayyed Mahdi Hejazi
  Isfahan University of Technology

Abstract

Many studies have been done on the stabilization of weak soil using conventional chemical stabilizers such as lime, cement as well as modern materials such as nanoparticles; however, very few studies have examined the effect of coated fibers on the strength of stabilized soil. This paper presents the results of a series of direct shear tests on soil specimens treated with ceramic fiber, nanosilica, and kaolin. The effects of ceramic fibers, fiber length, nanosilica, and kaolin on the mechanical characteristics and shear strength of silty sand was investigated. The results show that the addition of fiber to silty sand resulted in a significant increase in the strength of the soil specimens. The dilative behavior of the soil specimen decreased with the addition of ceramic fibers. The cohesion of the fiber-reinforced specimens increased when the fiber surface was coated with nanosilica or kaolin particles. The friction angle of the coated fiber-reinforced specimens decreased with the addition of nanosilica particles; however, the friction angle of the coated fiber-reinforced specimens was practically independent of the kaolin content.

1. Introduction

Techniques such as conventional stabilization and natural or synthetic fiber reinforcement have been proposed for soil improvement. Studies have shown that conventional stabilizers such as cement and lime and reinforcing materials such as natural or synthetic fibers can be used to strengthen and improve the mechanical behavior, hydraulic properties and freeze-thaw durability and reduce the swelling potential of geotechnical materials (Consoli et al. 2009; Kalantari et al. 2011; Hejazi et al. 2012; Asgari et al. 2015; Abdi and Mirzaeifar 2016; Yasui et al. 2016; Lv et al. 2018; Louzada et al. 2019; Saadat and Bayat 2019; Meeravali et al. 2020; Lu et al. 2020).

A number of studies have examined the mechanical properties of fiber-reinforced soil (Toé Casagrande et al. 2006; Plé and Lê 2012; Anagnostopoulos et al. 2013; Correia et al. 2017; Mirzababaei et al. 2018; Faghih Khorasani and Kabir 2020; Chebbi et al. 2020; Liu et al. 2020). Polypropylene, steel, basalt, glass, carpet-waste, tire, and carbon fibers have all been extensively studied for soil reinforcement (Akbulut et al. 2007; Orakoglu et al. 2017; Boz and Sezer 2018; Lv et al. 2018, 2019).

Although many studies have examined the mechanical characteristics of fiber-reinforced soil, none have examined the effect of nanosilica- or kaolin-coated ceramic fibers on the mechanical characteristics of soil. Ceramic fiber comprises inorganic, small-dimension filaments or threads composed of ceramic material that are lightweight, resistant to high temperatures, has low thermal conductivity, a high elastic modulus, and is highly resistant to corrosion caused by acid, alkali, and salt. The use of ceramic fiber in casting shells (Huang et al. 2019), cement mortar (Ma et al. 2005), and concrete (Su and Xu 2013; Siddique et al. 2019) has been reported; however, no investigations could be found in the literature on the use of ceramic fiber for soil stabilization.

Nanotechnology has evolved rapidly over the past twenty years. Nanomaterials have been used in a variety of fields since their introduction in 1959. Studies have shown that the use of nanomaterials in

geotechnical construction can improve the mechanical behavior and physical and chemical characteristics of weak soil (Sameni et al. 2015; Huang and Wang 2016; Kim et al. 2016; Lin et al. 2016; Iranpour and haddad 2016; Sarli et al. 2020; Zidi et al. 2020). Taha and Taha (2012) indicated that the addition of nano-Al_2O_3 to soil decreased both the expansive and shrinkage strains.

Cui et al. (2018) studied the shear strength parameters and microstructure of silty sand treated with carbon fiber and nanosilica. They reported that the shear strength parameters of specimens significantly increased with the addition of carbon fiber and nanosilica. The addition of carbon fiber to soil increased both the friction angle and cohesion; however, the nanosilica increased only the cohesion. Sarli et al. (2020) indicated that the addition of recycled polyester and nano-SiO_2 to loess soil increased its shear strength.

Previous studies showed that kaolin can be used to partially replace cement in in mortar and concrete, which can reduce energy consumption during cement production and is environmentally friendly (Sabir et al. 2001; Samet et al. 2007; Gonçalves et al. 2009; Shafiq et al. 2015). Wong et al. (2013) used kaolin as an additive for stabilization of peat soil. The results indicated that the specimen containing 10% kaolin as cement replacement had the highest strength.

The current study investigated the mechanical characteristics of reinforced silty sand containing ceramic fibers coated with nanomaterial or kaolin particles as a new stabilizer. The novelty of the current study includes the coating of the ceramic fibers with nanosilica or kaolin particles in order to improve the interfacial interaction of the fiber matrix. A series of direct shear tests was performed to determine the effect of the fiber content and length, and nanosilica or kaolin content on the mechanical characteristics of the stabilized specimens. The interaction between the soil particles and fiber and/or nanosilica- or kaolin-coated fibers was examined using scanning electron microscopy (SEM).

2. Materials And Experimental Procedure

2.1. Materials

The soil was collected from the Sejzi industrial zone to the east of the city of Isfahan in Iran. Fig. 1 shows the grain-size distribution curve and an image of the soil. Table 1 lists the physical and geotechnical properties of the soil. The modified Proctor compaction test was used to assess the maximum dry density (MDD) and optimum moisture content (OMC) according to ASTM D-1557. The soil was classified as silty sand (SM) according to the Unified Soil Classification System.

Tables 2 and 3 show the physical properties and chemical composition of the ceramic fibers, respectively. The ceramic fibers consisted of melted and blown kaolin melt with a high percentage of a mixture of pure alumina powder and mixed silica. After melting and blowing the kaolin melt in a furnace at 2000°C, the alumina and silica mixture was blown in by compressed air. These fibers were white, flexible, and had lengths of up to 50 mm and diameters of 2 to 3 µm.

Tables 4 and 5 present the physical and chemical characteristics of the hydrophilic nanosilica and kaolin particles, respectively. Kaolin is a subgroup of clay that consists of alternate layers of silica and alumina. These form natural morphologies such as hexagonal platelets, rolled sheets and tubes (Wong et al. 2013). Table 6 lists the physical properties of the adhesive.

2.2. Testing program

The mechanical characteristics of silty sand treated with nanosilica- or kaolin-coated ceramic fiber was investigated by direct shear testing. The effects of the ceramic fiber content and length, and the nanosilica and kaolin contents on the mechanical characteristics of specimens were determined. Table 7 summarizes the details of the direct shear tests. The first group of the tests evaluated the effects of the addition of ceramic fiber and the fiber length on the mechanical behavior of the reinforced specimens. The second and third groups examined the effects of the nanosilica and kaolin contents, respectively. The fourth and fifth groups of tests examined the effects of fiber content and length, and the nanosilica and kaolin contents on the mechanical characteristics of the specimens treated with ceramic fibers coated with nanosilica or kaolin particles, respectively. SEM images were used to examine the microstructure of the composites.

2.3. Specimen preparation

When preparing the specimens, the required amount of soil was dried in an oven for at least 24 h at approximately 110°C. Afterward, the amount of ceramic fiber required for the fiber-reinforced specimens was mixed until a uniform distribution of the ceramic fiber was achieved in the mixture. Finally, the water was added to the mixture up to the optimum moisture content (OMC) and mixed until the mixture was uniformly moist. The specimens containing nanosilica or kaolin were prepared using a procedure similar to that used for ceramic fiber-reinforced specimens.

Nanosilica- or kaolin-coated ceramic fibers were created using an adhesive material. The fiber coating increased the resistance of the fibers to fire and environmental effects. When preparing the specimens containing coated fibers, the required amount of ceramic fibers was weighed and then the adhesive was sprayed onto their surfaces. During spraying, the ceramic fibers were rotated to assure that all surfaces of the fibers were coated. The spraying time for each 0.5% of ceramic fibers was held constant at 15 s. Every attempt was made to spread the adhesive homogeneously onto the surfaces of the ceramic fibers. Next, the required amount of nanosilica or kaolin was sprayed onto the surfaces of the ceramic fibers. After the ceramic fiber coating was prepared with an adhesive layer, the nanosilica or kaolin particles were mixed with the dry soil. Finally, the required amount of water was added to the composite up to the OMC of the soil. All specimens were prepared at the OMC and MDD of the soil.

2.4. Testing apparatus

A direct shear test measures the shear strength properties of cohesion and the friction angle of the soil. In this study, a series of direct shear tests was conducted on the specimens according to ASTM D3080. The

required amount of composite was poured into the shear box and then was compacted to achieve the MDD. The shear box had dimensions of 100 × 100 mm at a constant horizontal displacement rate of 0.2 mm/min. Three direct shear tests were conducted for each composite at three normal stress values (0.1, 0.2, and 0.3 MPa). The shear stress–shear strain curve, vertical strain-shear strain curve, cohesion, and friction angle of the composite were obtained from direct shear tests.

3. Tests Results And Discussion

3.1. Direct shear tests results

The results of the direct shear tests on the natural soil specimens are presented in Fig. 2. As shown, the natural soil exhibited dilative behavior. Fig. 3 shows the response of the ceramic-fiber-reinforced specimens at a fiber content of 0.5% (by dry weight of soil) and fiber lengths of 6, 12, and 18 mm. The results show that the addition of ceramic fiber to the natural soil significantly increased the shear strength of the reinforced soil at any fiber length. These results are in good agreement with those of previous studies on fiber-reinforced soil (Sadek et al. 2010, Hamidi and Hooresfand 2013, Zhang et al. 2017, Faghih Khorasani and Kabir 2020). The ceramic fiber-reinforced specimens exhibited less dilative behavior than the natural soil specimens. This is likely the result of the increase in spatial confinement caused by ceramic-fiber reinforcement. This also is in agreement with the response observed in previous studies for the soils reinforced with other fiber types (Noorzad and Zarinkolaei 2015, Choobbasti et al. 2019). An increase in the ceramic fiber length caused a decrease in the dilative behavior.

In general, the peak shear strength of the specimens increased with an increase in the normal stress. The peak shear strength of the ceramic-fiber-reinforced specimens occurred at a higher shear strain level compared to the natural soil specimens. The influence of the increase of fiber length did not show a regular effect on the peak shear strength. In other words, it had a dual influence on the peak shear strength depending on the normal stress. For the reinforced specimens, there was a clear trend of increase in strain with an increase in the fiber length at the peak shear stress. The shorter fibers provided better fiber orientation and dispersion because there were more of them at a given fiber content than for the longer fibers. This had a direct influence on the strain at peak shear stress and resulted in greater adhesion strength between the fibers and the matrix.

The effects of nanosilica content and kaolin content on the response of the specimens stabilized with additive contents of 0.1% and 0.5% (dry weight of soil) are shown in Figs. 4 and 5, respectively. As shown, the shear strength increased with the addition of nanosilica or kaolin particles to the soil. The specimens containing kaolin particles had a greater shear strength than the specimens containing nanosilica particles at a given additive content. The nanosilica- and kaolin-stabilized specimens appeared to be less dilative (or more contractive) than the natural soil specimens. This was due to strong and sufficient bonding between the soil particles and additive particles.

The addition of water to the mixture caused a viscous gel to be produced by the nanosilica or kaolin particles that bound the soil particles together and filled the voids between the soil particles. This led to

an increase in the shear strength. The peak shear strength of the specimens stabilized with nanosilica or kaolin particles occurred at a higher shear strain level compared to the natural soil specimens. However, the shear strength decreased with an increase in the nanosilica content from 0.1% to 0.5%.

Fig. 6 shows the cohesion and friction angle of the specimens. It can be seen that both parameters increased with the addition of ceramic fiber, nanosilica or kaolin particles to the soil. The specimen containing 0.5% kaolin particles had the highest cohesion value at 1.32 MPa. The specimens containing 0.5% ceramic fiber had the lowest value at about 0.24 MPa. These values were almost independent of the kaolin content and fiber length.

The friction angle increased sharply to the maximum values for specimens containing ceramic fiber or kaolin particles. The friction angle was independent of fiber length or kaolin content, however, an increase in the nanosilica content from 0.1% to 0.5% caused a decrease in the friction angle and an increase in cohesion. Increasing the nanosilica content increased the cohesion, but decreased the friction angle, which is in good agreement with the results reported by Cui et al. (2018). The total shear strength decreased significantly with an increase in the nanosilica content from 0.1% to 0.5% because the rate of decrease in the friction angle was greater than the rate of increase in cohesion. The increase in cohesion was related to the pore-filling influence of the viscous gel produced by the nanosilica. The decrease in the friction angle could be related to the presence of small particles producing less friction and the excessive agglomeration of nanosilica, as has been explained by Cui et al. (2018).

The responses of specimens containing ceramic fiber and nanosilica particles are presented in Figs. 7 to 9. The results show that the specimens containing 0.1% nanosilica exhibited more shear strength than those of containing 0.5% nanosilica. The specimens containing 0.5% nanosilica exhibited less dilation than those of containing 0.1% nanosilica at any fiber length. Figs. 10 to 12 show the responses of specimens containing ceramic fiber and kaolin particles and reveal that the specimens containing 0.5% kaolin exhibited more shear strength than those containing 0.1% kaolin at any fiber length. The effect of the addition of kaolin on the volumetric behavior of the ceramic-fiber-reinforced specimens varied according to the fiber length.

Fig. 13 presents the cohesion and friction angle versus the nanosilica or kaolin contents for different fiber lengths. Coating the fibers with nanosilica increased the cohesion, but decreased the friction angle. The total shear strength decreased with an increase in the nanosilica content used in the coating from 0.1% to 0.5%. This occurred because the rate of decrease in the friction angle was greater than the rate of increase in cohesion. The increase in cohesion was related to the viscous gel covering the fiber surfaces, however, this viscous gel covering did not improve the interfacial bond properties and decreased the friction between the soil particles and fiber surfaces.

The shear strength envelopes for the specimens at peak shear stress are shown in Fig. 14. It can be seen that the cohesion of the fiber-reinforced specimens increased with the addition of nanosilica or kaolin particles. The increase in cohesion caused by the ceramic fiber coating was more pronounced for the

specimens containing kaolin particles. The cohesion increased with an increase in the fiber length from 6 to 18 mm at a given nanosilica or kaolin content.

The friction angle of the fiber-reinforced specimens decreased with the addition of nanosilica particles. In other words, the friction between the soil particles and ceramic fiber surfaces decreased after the fibers were coated with nanosilica. In contrast to the uncoated ceramic fibers, which have a smooth surface, the coated ceramic fibers showed different surface characteristics. These included the type of coating (nanosilica or kaolin), being fiber wrapped, or having a deformed ribbed surface that provided a bond with the soil. However, the friction angle of the fiber-reinforced specimens was almost independent of the kaolin content. The effect of fiber length on the friction angle of the fiber-reinforced specimens varied in the specimens containing nanosilica and kaolin particles.

3.2. SEM analysis

The fiber−soil interaction in reinforced soil is complicated, especially at the microscopic scale. Tang et al. (2007) indicated that the binding material properties, applied stress condition, surface roughness of the fibers, and contact between the fibers and soil particles are the major parameters which govern the micro-mechanical characteristics of the fiber-soil interface. In this work, after shearing, a number of specimens were analyzed using SEM. The SEM micrographs of the kaolin and nanosilica particles, ceramic fibers, and specimens reinforced with ceramic fibers coated by nanosilica or kaolin are shown in Figs. 15 and 16. It can be seen that the kaolin particles are more angular than the nanosilica particles.

The SEM micrographs show that the surfaces of the ceramic fibers were clean and smooth. When the fibers were coated with nanosilica or kaolin, some particles clung to the ceramic fiber surface and formed an interlock which improved the interactions between the ceramic fiber and the sand particles. The SEM images show that the ceramic fiber surface coated with kaolin contributed to the bond strength, but the nanosilica particles were less angular than the kaolin particles. It can be concluded that the fibers coated with kaolin were able to provide much greater pull-out resistance than the same fibers coated with nanosilica.

4. Conclusions

In this study, a series of direct shear tests was conducted to investigate the effects of the addition of ceramic fibers and the fiber length, nanosilica content, and kaolin content on the mechanical behavior of silty sand. The test results produced the following conclusions.

It was observed that both the cohesion and friction angle increased with the addition of ceramic fiber, nanosilica, or kaolin particles to the natural soil. The shear strength of the specimens increased and the dilative potential decreased with the addition of ceramic fibers. The ceramic fiber length had no significant effect on the shear strength parameters of the reinforced specimens.

The shear strength increased with the addition of nanosilica or kaolin particles to the soil. The specimens containing kaolin particles had more shear strength than the specimens containing nanosilica particles at a given additive content. The nanosilica or kaolin stabilized specimens appeared to be less dilative (or more contractive) than the natural soil specimens.

The friction angle also was independent of the kaolin content; however, an increase in the nanosilica content from 0.1–0.5% caused a decrease in the friction angle and an increase in cohesion. The cohesion of the fiber-reinforced specimens increased when the fiber surface was coated with nanosilica or kaolin particles. The increase in cohesion after coating the ceramic fibers was more pronounced for specimens containing kaolin particles. The friction angle of the coated fiber-reinforced specimens decreased with the addition of nanosilica particles; however, the friction angle of coated-fiber-reinforced specimens was almost independent of the kaolin content. The effect of fiber length on the friction angle of the coated-fiber-reinforced specimens varied in the specimens containing nanosilica and kaolin particles.

Declarations

Funding

No Found

Conflicts of interest/Competing interests

The authors declare no competing interests

Availability of data and material

No data, models, or codes were generated or used during the study.

References

1. Abdi MR, Mirzaeifar H (2016) Effects of discrete short polypropylene fibers on behavior of artificially cemented kaolinite. Int J Civ Eng 14:253–262. doi: 10.1007/s40999-016-0022-5

2. Akbulut S, Arasan S, Kalkan E (2007) Modification of clayey soils using scrap tire rubber and synthetic fibers. Appl Clay Sci 38:23–32. doi: 10.1016/j.clay.2007.02.001

3. Anagnostopoulos CA, Papaliangas TT, Konstantinidis D, Patronis C (2013) Shear Strength of Sands Reinforced with Polypropylene Fibers. Geotech Geol Eng 31:401–423. doi: 10.1007/s10706-012-9593-3

4. Asgari MR, Baghebanzadeh Dezfuli A, Bayat M (2015) Experimental study on stabilization of a low plasticity clayey soil with cement/lime. Arab J Geosci 8:1439–1452. doi: 10.1007/s12517-013-1173-1

5. Boz A, Sezer A (2018) Influence of fiber type and content on freeze-thaw resistance of fiber reinforced lime stabilized clay. Cold Reg Sci Technol 151:359–366. doi: 10.1016/j.coldregions.2018.03.026

6. Chebbi M, Guiras H, Jamei M (2020) Tensile behaviour analysis of compacted clayey soil reinforced with natural and synthetic fibers: effect of initial compaction conditions. Eur J Environ Civ Eng 24:354–380. doi: 10.1080/19648189.2017.1384762

7. Choobbasti AJ, Kutanaei SS, Ghadakpour M (2019) Shear behavior of fiber-reinforced sand composite. Arab J Geosci 12:1–6. doi: 10.1007/s12517-019-4326-z

8. Consoli NC, Da Silva Lopes L, Foppa D, Heineck KS (2009) Key parameters dictating strength of lime/cement-treated soils. Proc Inst Civ Eng Geotech Eng 162:111–118. doi: 10.1680/geng.2009.162.2.111

9. Correia AAS, Venda Oliveira PJ, Teles JMNPC, Pedro AMG (2017) Strength of a stabilised soil reinforced with steel fibres. Proc Inst Civ Eng Geotech Eng 170:312–321. doi: 10.1680/jgeen.16.00200

10. Cui H, Jin Z, Bao X, et al (2018) Effect of carbon fiber and nanosilica on shear properties of silty soil and the mechanisms. Constr Build Mater 189:286–295. doi: 10.1016/j.conbuildmat.2018.08.181

11. Faghih Khorasani F, Kabir MZ (2020) The effectiveness of rubber short fibers reinforcing on mechanical characterization of clay adobe elements under static loading. Eur J Environ Civ Eng. doi: 10.1080/19648189.2020.1751302

12. Gonçalves JP, Tavares LM, Toledo Filho RD, Fairbairn EMR (2009) Performance evaluation of cement mortars modified with metakaolin or ground brick. Constr Build Mater 23:1971–1979. doi: 10.1016/j.conbuildmat.2008.08.027

13. Hamidi A, Hooresfand M (2013) Effect of fiber reinforcement on triaxial shear behavior of cement treated sand. Geotext Geomembranes 36:1–9. doi: 10.1016/j.geotexmem.2012.10.005

14. Hejazi SM, Sheikhzadeh M, Abtahi SM, Zadhoush A (2012) A simple review of soil reinforcement by using natural and synthetic fibers. Constr Build Mater 30:100–116. doi: 10.1016/j.conbuildmat.2011.11.045

15. Huang P, Lu G, Yan Q, Mao P (2019) Effect of ceramic and nylon fiber content on composite silica sol slurry properties and bending strength of investment casting shell. Materials (Basel) 12:. doi: 10.3390/ma12172788

16. Huang Y, Wang L (2016) Experimental studies on nanomaterials for soil improvement: a review. Environ Earth Sci 75:1–10. doi: 10.1007/s12665-015-5118-8

17. Iranpour B, haddad A (2016) The influence of nanomaterials on collapsible soil treatment. Eng Geol 205:40–53. doi: 10.1016/j.enggeo.2016.02.015

18. Kalantari B, Prasad A, Huat BBK (2011) Stabilising peat soil with cement and silica fume. Proc Inst Civ Eng Geotech Eng 164:33–39. doi: 10.1680/geng.900044

19. Kim SA, Kamala-Kannan S, Oh SG, et al (2016) Simultaneous removal of chromium(VI) and Reactive Black 5 using zeolite supported nano-scale zero-valent iron composite. Environ Earth Sci 75:1–8. doi: 10.1007/s12665-015-4855-z

20. Lin DF, Luo HL, Hsiao DH, et al (2016) Enhancing soft subgrade soil with a sewage sludge ash/cement mixture and nano-silicon dioxide. Environ Earth Sci 75:1–11. doi: 10.1007/s12665-016-

5432-9

21. Liu L, Li Z, Cai G, et al (2020) Evaluating the influence of moisture on settling velocity of road embankment constructed with recycled construction wastes. Constr Build Mater 241:117988. doi: 10.1016/j.conbuildmat.2019.117988

22. Louzada NDSL, Malko JAC, Casagrande MDT (2019) Behavior of Clayey Soil Reinforced with Polyethylene Terephthalate. J Mater Civ Eng 31:. doi: 10.1061/(ASCE)MT.1943-5533.0002863

23. Lu Y, Liu S, Zhang Y, et al (2020) Freeze-thaw performance of a cement-treated expansive soil. Cold Reg Sci Technol 170:102926. doi: 10.1016/j.coldregions.2019.102926

24. Lv Q, Chang C, Zhao B, Ma B (2018) Loess Soil Stabilization by Means of SiO2 Nanoparticles. Soil Mech Found Eng 54:409–413. doi: 10.1007/s11204-018-9488-2

25. Lv X, Zhou H, Liu X, Song Y (2019) Experimental study on the effect of basalt fiber on the shear behavior of cemented sand. Environ Earth Sci 78:1–13. doi: 10.1007/s12665-019-8737-7

26. Ma Y, Zhu B, Tan M (2005) Properties of ceramic fiber reinforced cement composites. Cem Concr Res 35:296–300. doi: 10.1016/j.cemconres.2004.05.017

27. Meeravali K, Alla S, Syed H, Ruben N (2020) An analysis of freeze-thaw cycles on geotechnical properties of soft-soil. Mater Today Proc 27:1304–1309. doi: 10.1016/j.matpr.2020.02.266

28. Mirzababaei M, Arulrajah A, Horpibulsuk S, et al (2018) Stabilization of soft clay using short fibers and poly vinyl alcohol. Geotext Geomembranes 46:646–655. doi: 10.1016/j.geotexmem.2018.05.001

29. Noorzad R, Zarinkolaei STG (2015) Comparison of mechanical properties of fiber-reinforced sand under triaxial compression and direct shear. Open Geosci 7:547–558. doi: 10.1515/geo-2015-0041

30. Orakoglu E, Liu J, Niu F, et al (2017) Dynamic behavior of fiber-reinforced soil under freeze-thaw cycles. Soil Dyn Earthq Eng 101:269–284. doi: 10.1016/j.soildyn.2017.07.022

31. Plé O, Lê TNH (2012) Effect of polypropylene fiber-reinforcement on the mechanical behavior of silty clay. Geotext Geomembranes 32:111–116. doi: 10.1016/j.geotexmem.2011.11.004

32. Saadat M, Bayat M (2019) Prediction of the unconfined compressive strength of stabilised soil by Adaptive Neuro Fuzzy Inference System (ANFIS) and Non-Linear Regression (NLR). Geomech Geoengin. doi: 10.1080/17486025.2019.1699668

33. Sabir B, Wild S, Bai J (2001) Metakaolin and calcined clays as pozzolans for concrete: A review. Cem Concr Compos 23:441–454. doi: 10.1016/S0958-9465(00)00092-5

34. Sadek S, Najjar SS, Freiha F (2010) Shear strength of fiber-reinforced sands. J Geotech Geoenvironmental Eng 136:490–499. doi: 10.1061/(ASCE)GT.1943-5606.0000235

35. Sameni A, Pourafshary P, Ghanbarzadeh M, Ayatollahi S (2015) Effect of nanoparticles on clay swelling and migration. Egypt J Pet 24:429–437. doi: 10.1016/j.ejpe.2015.10.006

36. Samet B, Mnif T, Chaabouni M (2007) Use of a kaolinitic clay as a pozzolanic material for cements: Formulation of blended cement. Cem Concr Compos 29:741–749. doi: 10.1016/j.cemconcomp.2007.04.012

37. Sarli JM, Hadadi F, Bagheri RA (2020) Stabilizing Geotechnical Properties of Loess Soil by Mixing Recycled Polyester Fiber and Nano-SiO2. Geotech Geol Eng 38:1151–1163. doi: 10.1007/s10706-019-01078-7

38. Shafiq N, Nuruddin MF, Khan SU, Ayub T (2015) Calcined kaolin as cement replacing material and its use in high strength concrete. Constr Build Mater 81:313–323. doi: 10.1016/j.conbuildmat.2015.02.050

39. Siddique S, Shrivastava S, Chaudhary S (2019) Influence of ceramic waste on the fresh properties and compressive strength of concrete. Eur J Environ Civ Eng 23:212–225. doi: 10.1080/19648189.2016.1275985

40. Su H, Xu J (2013) Dynamic compressive behavior of ceramic fiber reinforced concrete under impact load. Constr Build Mater 45:306–313. doi: 10.1016/j.conbuildmat.2013.04.008

41. Taha MR, Taha OME (2012) Influence of nano-material on the expansive and shrinkage soil behavior. J Nanoparticle Res 14:1–13. doi: 10.1007/s11051-012-1190-0

42. Tang C, Shi B, Gao W, et al (2007) Strength and mechanical behavior of short polypropylene fiber reinforced and cement stabilized clayey soil. Geotext Geomembranes 25:194–202. doi: 10.1016/j.geotexmem.2006.11.002

43. Toé Casagrande MD, Coop MR, Consoli NC (2006) Behavior of a fiber-reinforced bentonite at large shear displacements. J Geotech Geoenvironmental Eng 132:1505–1508. doi: 10.1061/(ASCE)1090-0241(2006)132:11(1505)

44. Wong LS, Hashim R, Ali F (2013) Improved strength and reduced permeability of stabilized peat: Focus on application of kaolin as a pozzolanic additive. Constr Build Mater 40:783–792. doi: 10.1016/j.conbuildmat.2012.11.065

45. Yasui K, Goto S, Kinoshita H, et al (2016) Ceramic waste glass fiber-reinforced plastic-containing filtering materials for turbid water treatment. Environ Earth Sci 75:1–11. doi: 10.1007/s12665-016-5933-6

46. Zhang T, Cai G, Liu S (2017) Application of lignin-based by-product stabilized silty soil in highway subgrade: A field investigation. J Clean Prod 142:4243–4257. doi: 10.1016/j.jclepro.2016.12.002

47. Zidi Z, Ltifi M, Ayadi Z Ben, et al (2020) Effect of nano-ZnO on mechanical and thermal properties of geopolymer. J Asian Ceram Soc 8:1–9. doi: 10.1080/21870764.2019.1693682

Tables

Table 1. Physical and geotechnical properties of soil

Values and descriptions	Characteristics
2.66	Specific gravity
20	Passing No. 200 sieve (%)
NP	Plasticity index (%)
SM	Unified Soil Classification System (USCS)
9.55	Optimum water content (%)
20.11	Maximum dry unit weight (kN/m^3)
0.01	Cohesion (MPa)
35.6	Friction angle (°)

Table 2. Physical properties of ceramic fiber

Property	Value
Cut length (mm)	6, 12 and 18
Filament diameter (μm)	3-5
Classification Temp. (°C)	1260
Non-Fibrous Content	<25%

Table 3. Chemical composition of ceramic fiber

Composition	Value
SiO_2	50-55
AL_2O_3	40-45
Fe_2O_3	<0.5
K_2O+Na_2O	<0.5

Table 4. Physical and chemical properties of nano-silica particles

Property/composition	Value
Specific surface area (m^2/g)	235
Main particle size (µm)	25
Agglomerate mean particle size (µm)	10.5
Tamped density (kg/m^3)	200
pH	6.8
SiO_2 (%)	>98.5
SO_3 (%)	0.5

Table 5. Physical and chemical properties of kaolin particles

Property/composition	Value
Specific gravity	2.57
Particle size (-2 µm) (%)	89
Liquid limit (%)	49.2
Plasticity index (%)	24.1
Specific surface area (m^2/g)	16.30
SiO_2 (%)	74.98
Al_2O_3 (%)	17.42
Fe_2O_3 (%)	9.54
TiO_2 (%)	0.96
CaO (%)	1.62
MgO (%)	0.29
P_2O_5 (%)	0.08

Table 6. Physical properties of adhesive

Property/composition	Values and descriptions
Solids Content (by wt.)	25%
Base	Synthetic Elastomers
Color (wet and dry)	Translucent
Spray Pattern	Low Mist, Fine Particle Spray
Spray Width	2" - 4"
Solvents	Acetone, Heptane, Cyclohexane
Flash Point	-42°F (-42°C)
Hazardous Air Pollutants (HAPS)	None

Table 7. A summary of the test details

Test Group	Ceramic fiber content (%)	Fiber length (mm)	Nano-silica content (%)	Kaolin content (%)
Group-1	0.5	6, 12 and 18	0	0
Group-2	0	0	0.1 and 0.5	0
Group-3	0	0	0	0.1 and 0.5
Group-4	0.5	6, 12 and 18	0.1 and 0.5	0
Group-5	0.5	6, 12 and 18	0	0.1 and 0.5

Figures
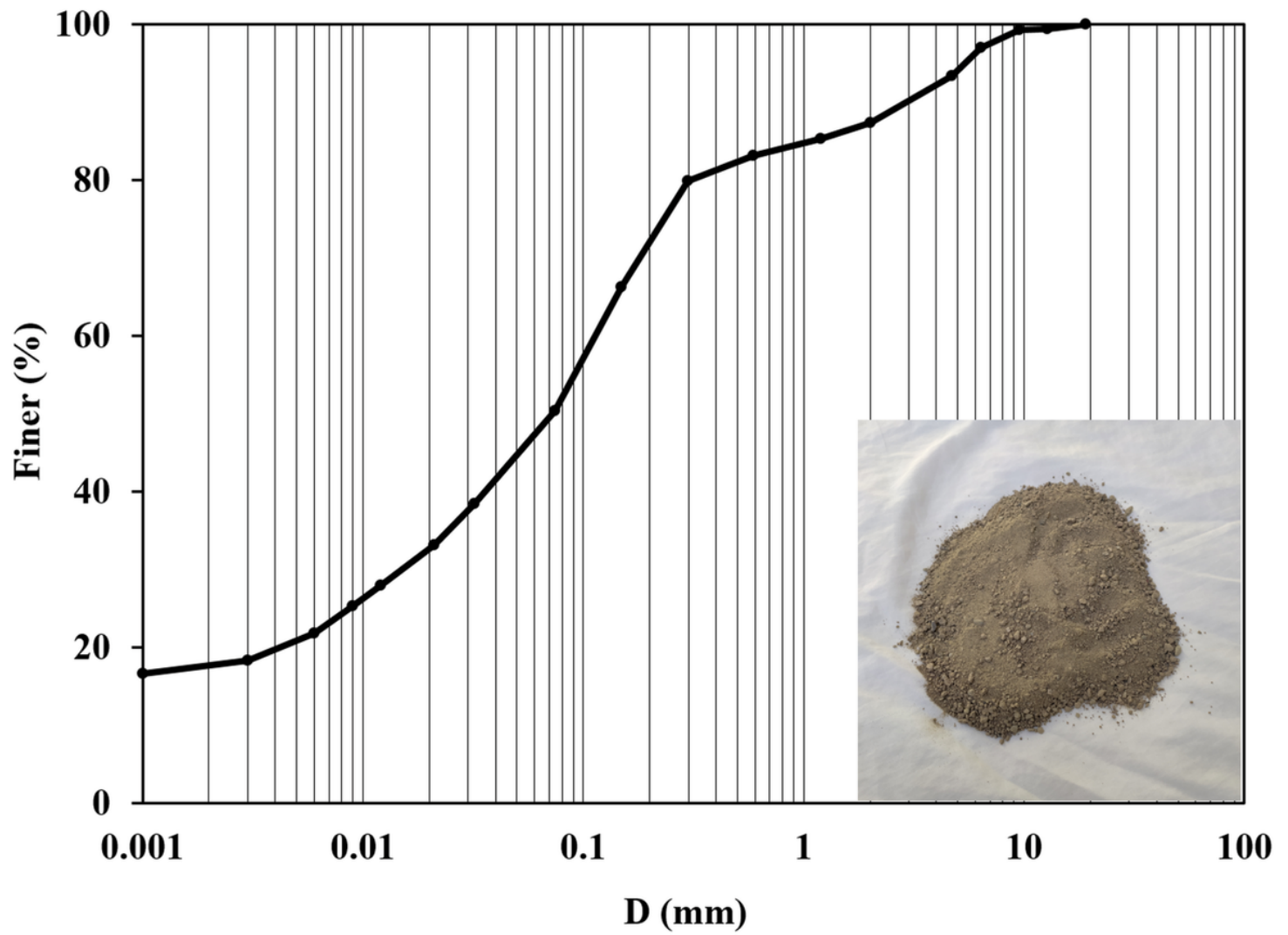
Figure 1

Grain size distribution curve and image of the soil.
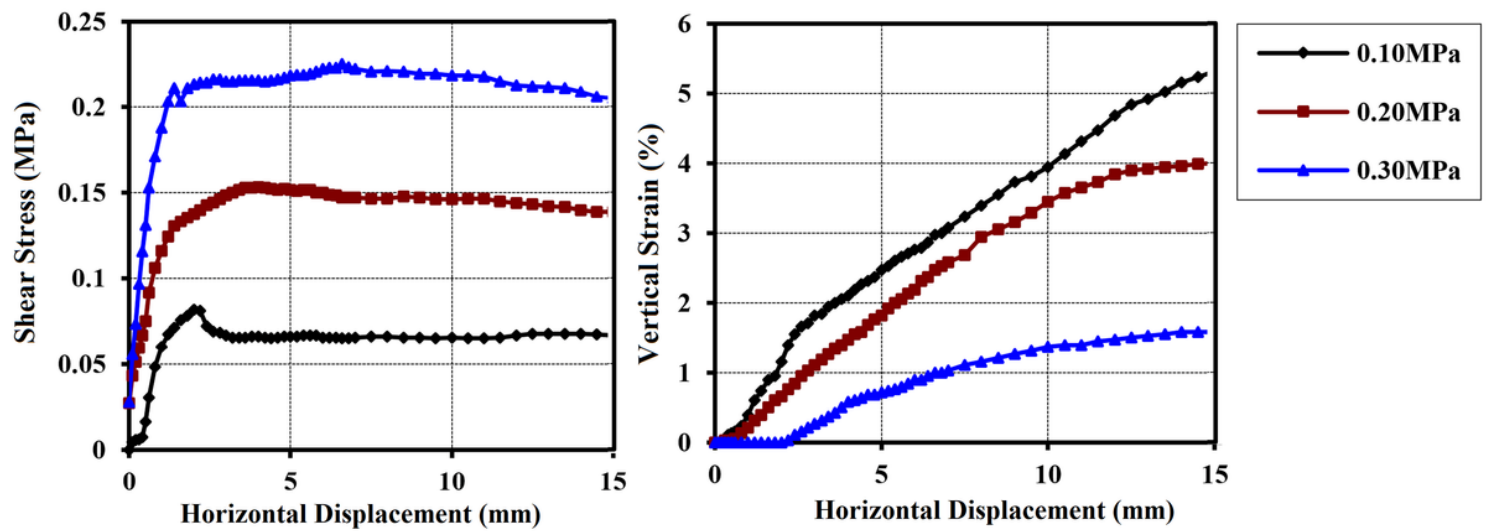
Figure 2

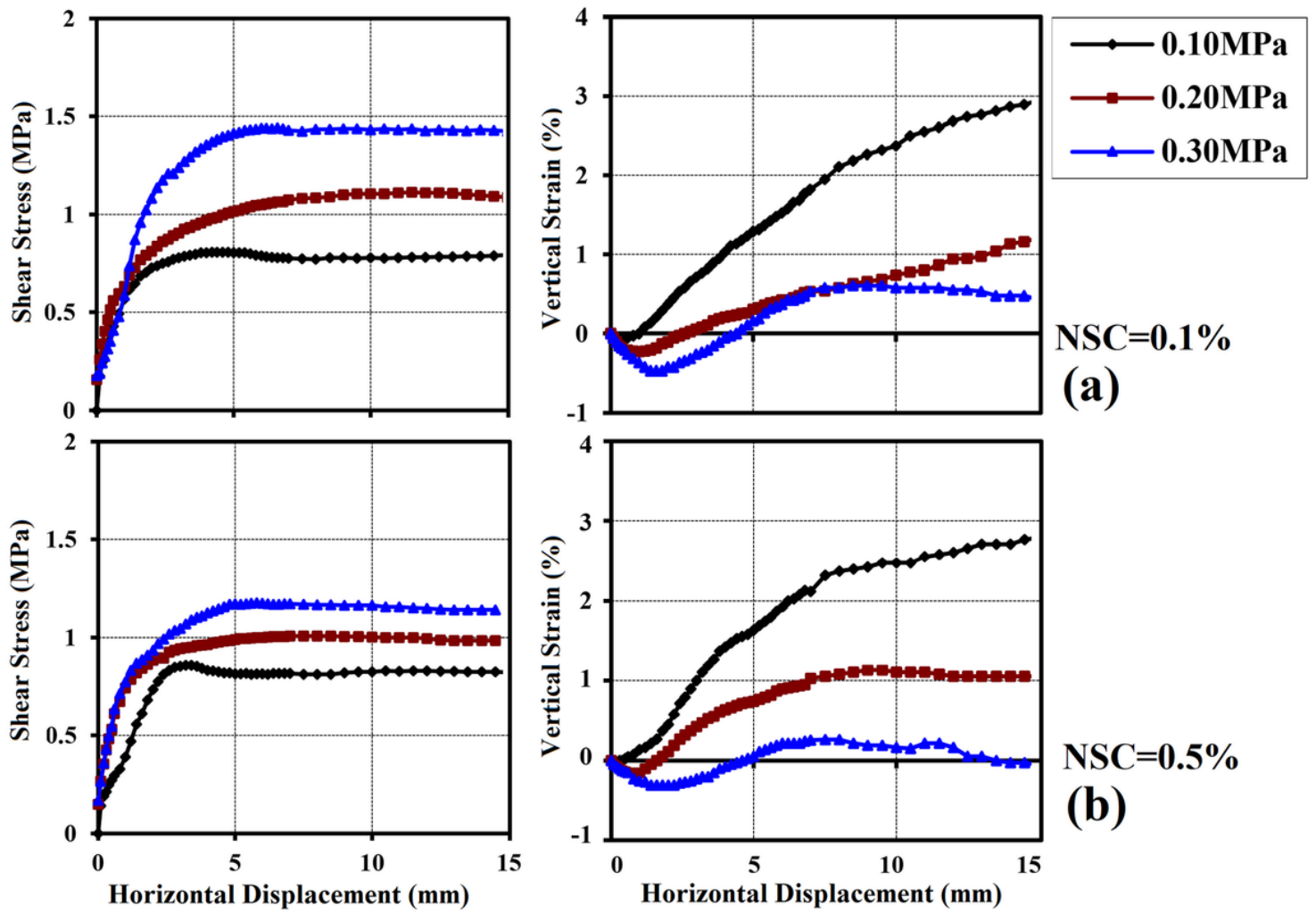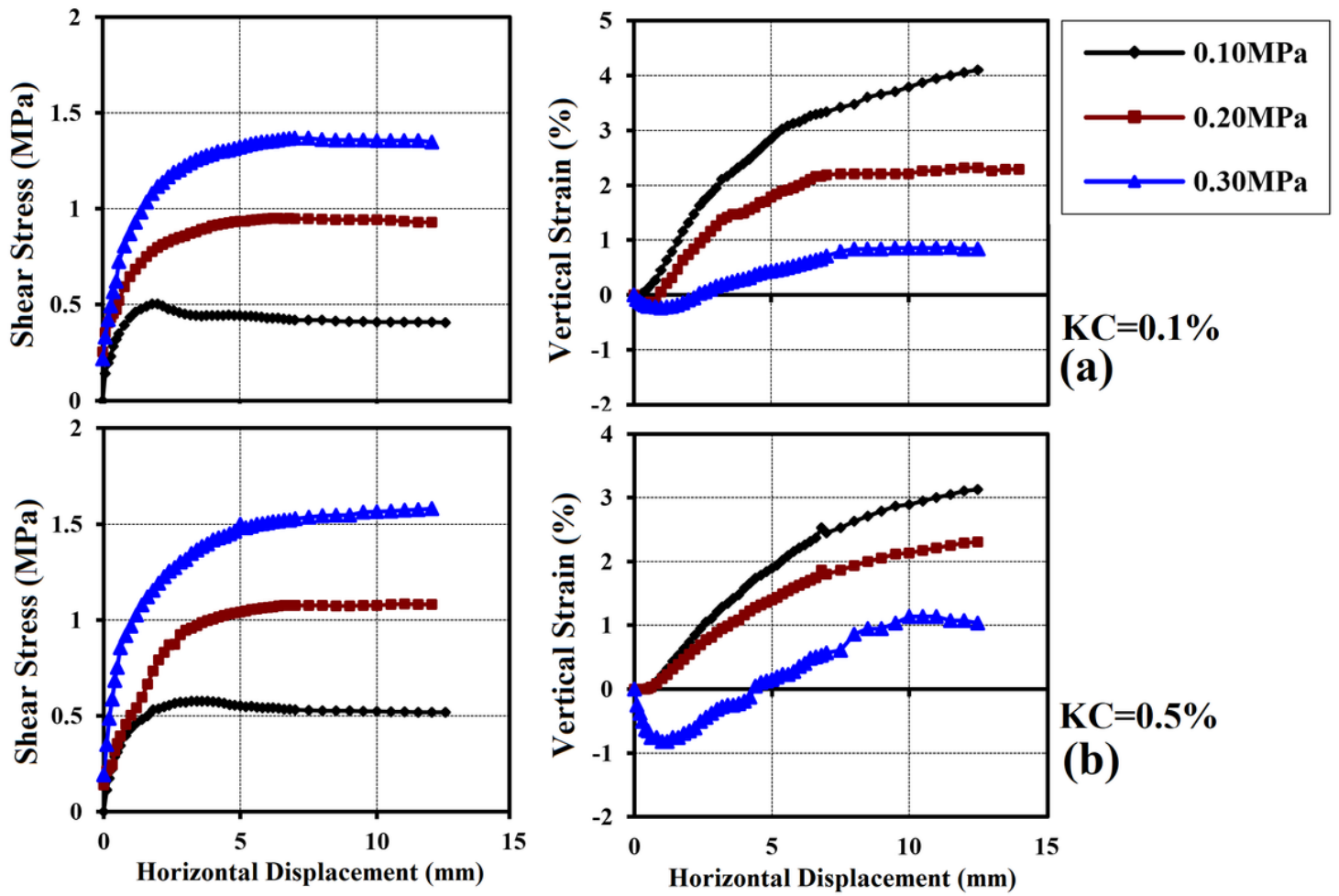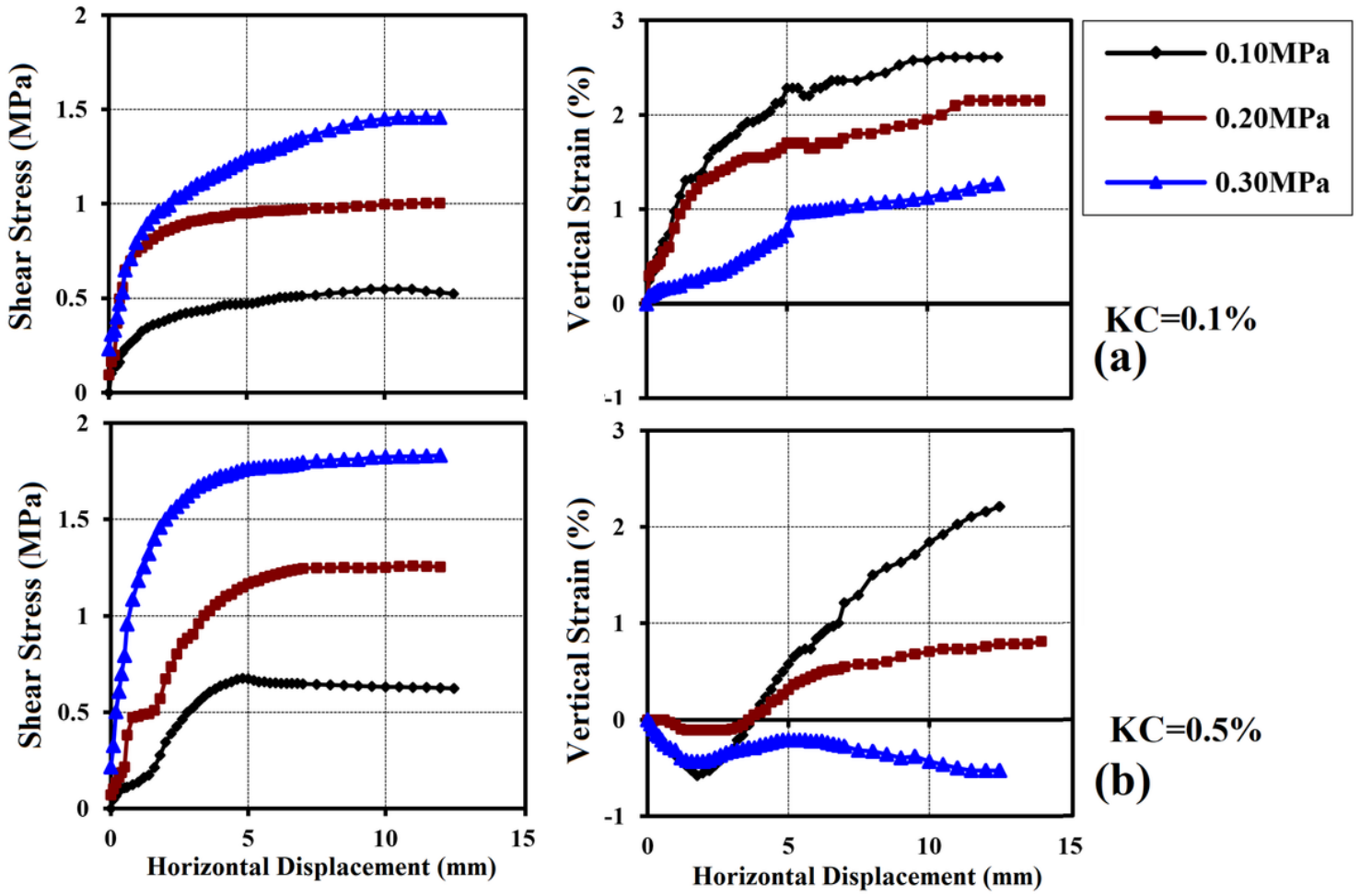Shear stress-shear strain and vertical strain-shear strain curves of the natural soil specimens.
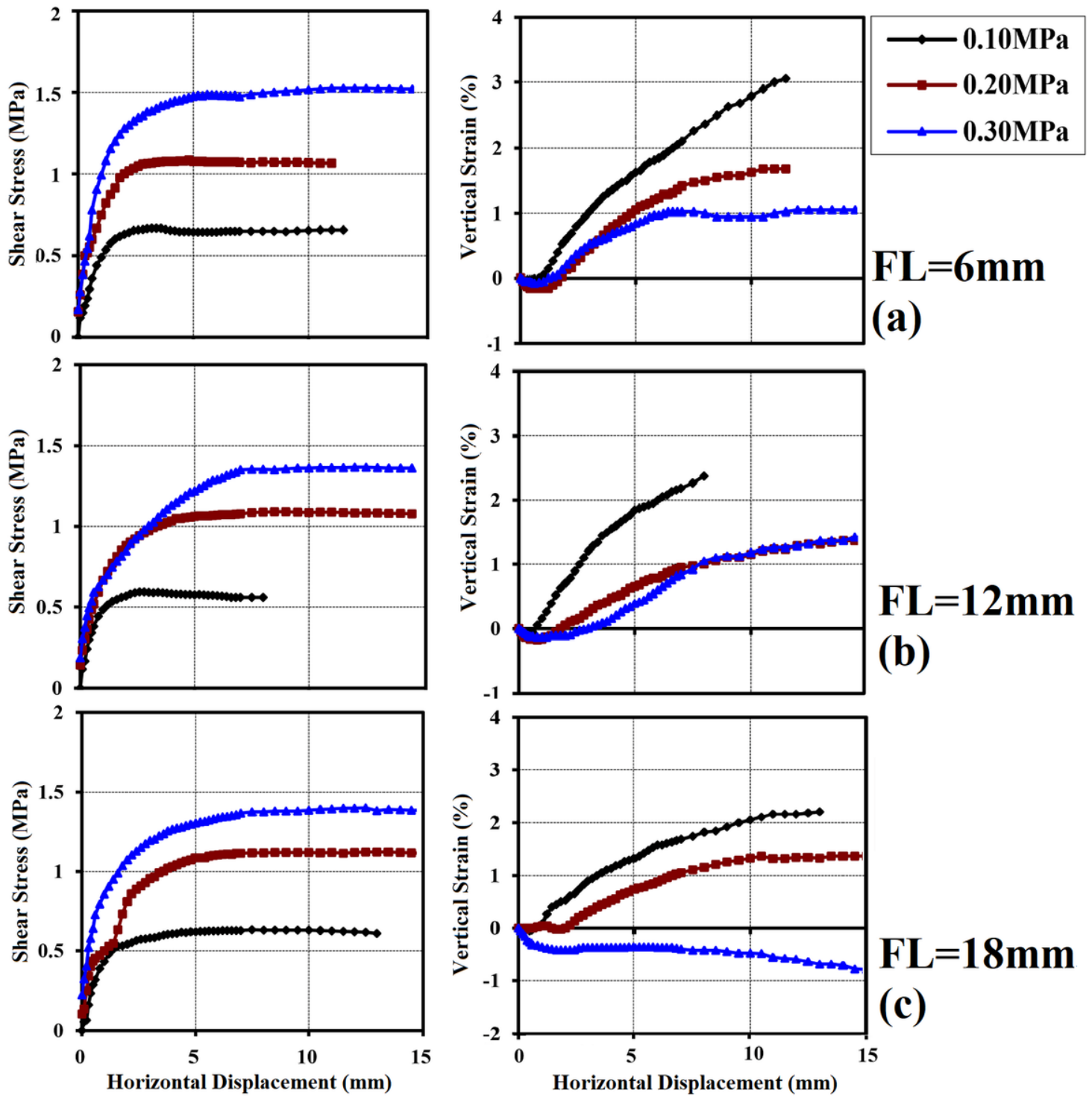
Figure 3

Shear stress-shear strain and vertical strain-shear strain curves of ceramic-fiber-reinforced specimens with a fiber content of 0.5% and fiber lengths of: (a) 6 mm, (b) 12 mm, (c)18 mm.
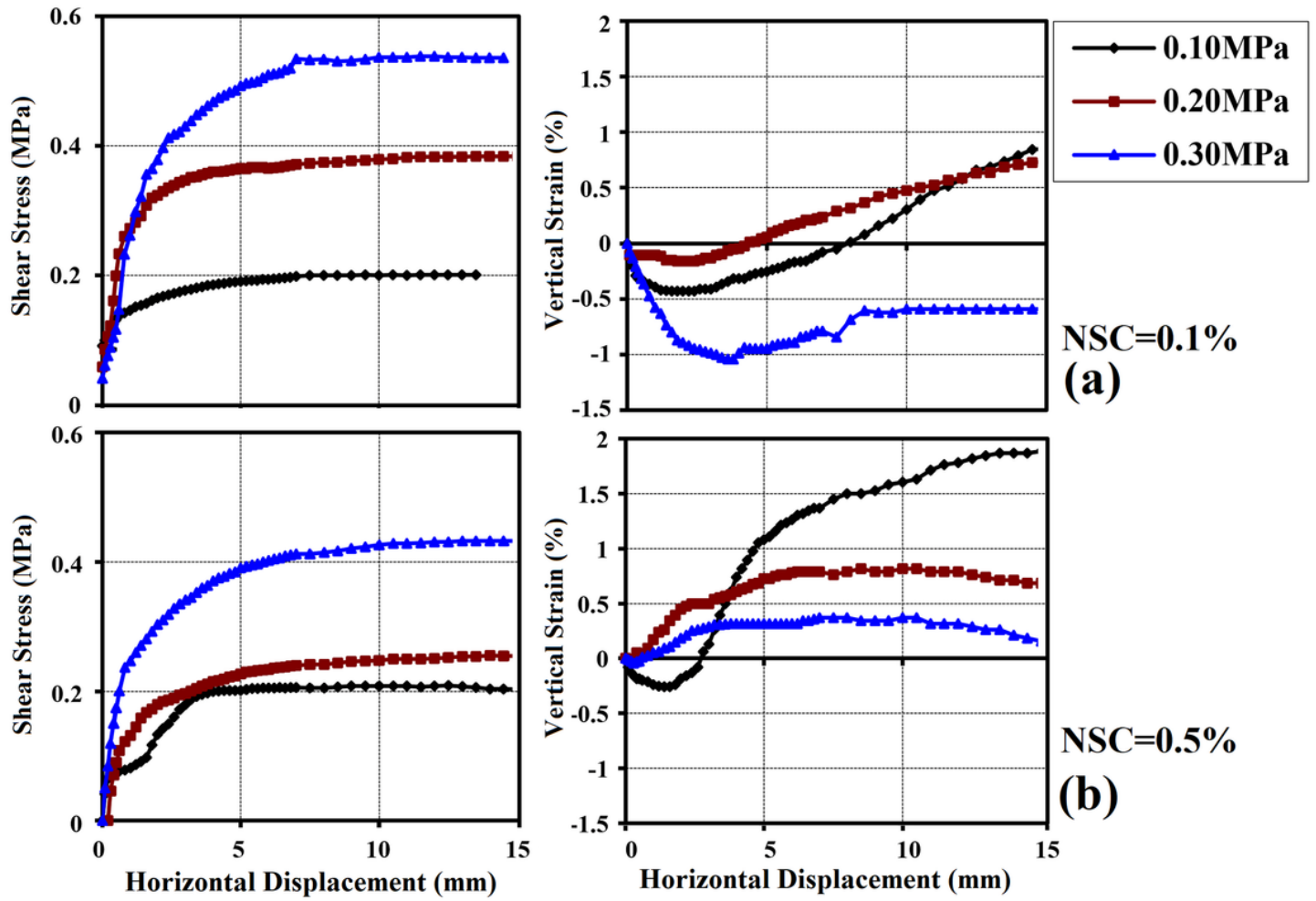
Figure 4

Shear stress-shear strain and vertical strain-shear strain curves of specimens with nanosilica contents of: (a) 0.1%, (b) 0.5%.
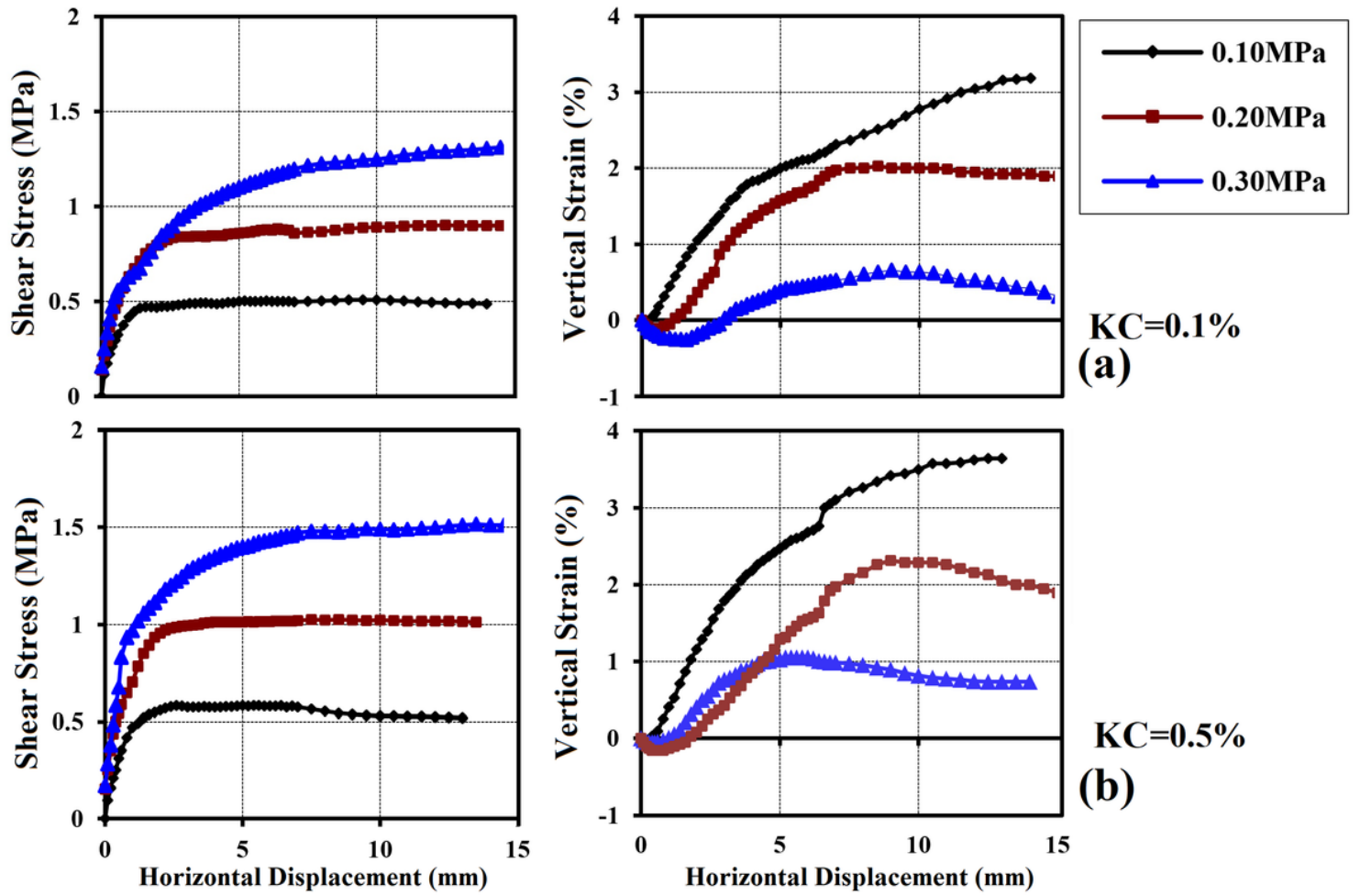
Figure 5

Shear stress-shear strain and vertical strain-shear strain curves of specimens with kaolin contents of: (a) 0.1%, (b) 0.5%.
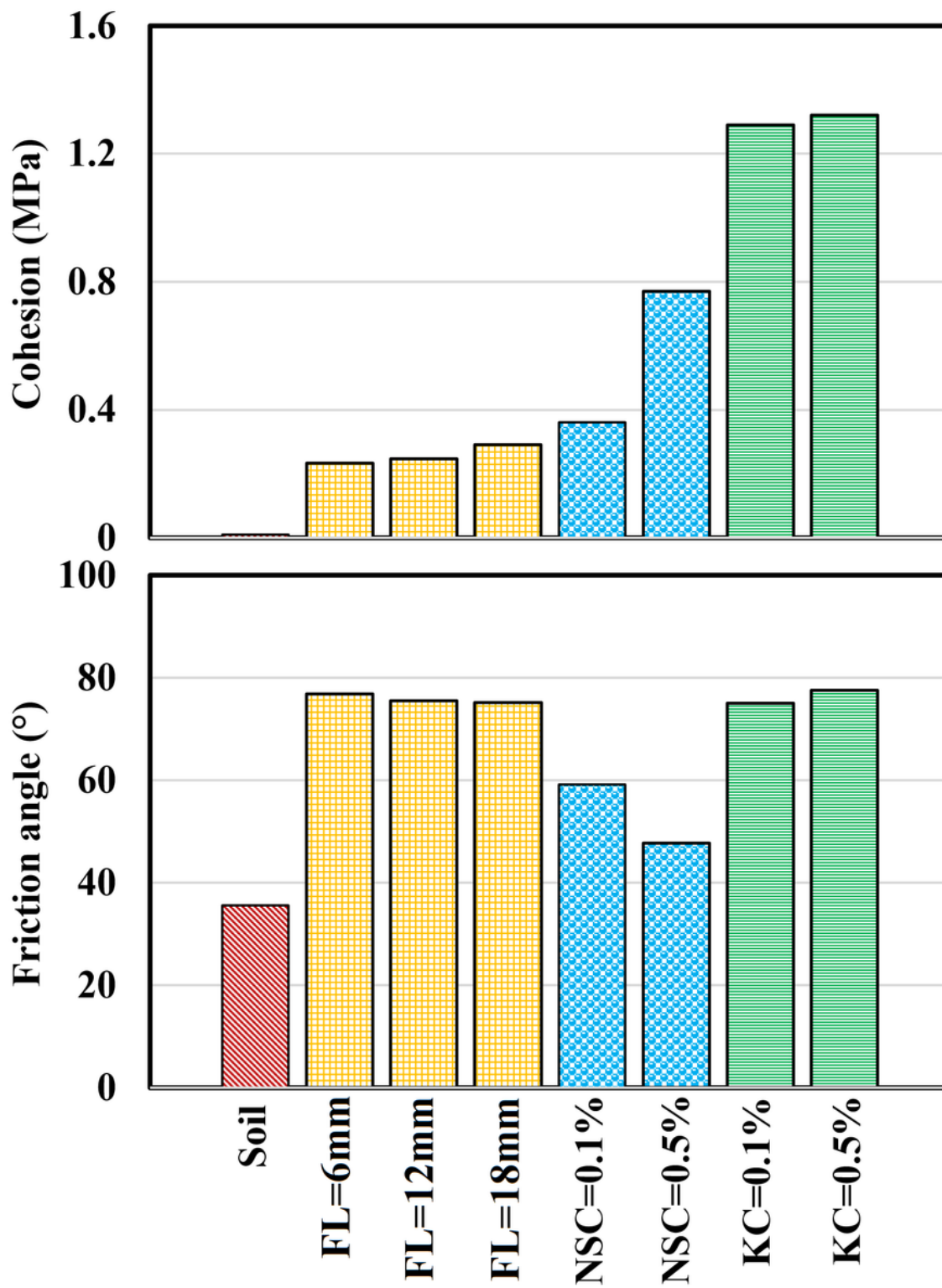
Figure 6

Effect of nanosilica and kaolin contents on the friction angle and cohesion of specimens.
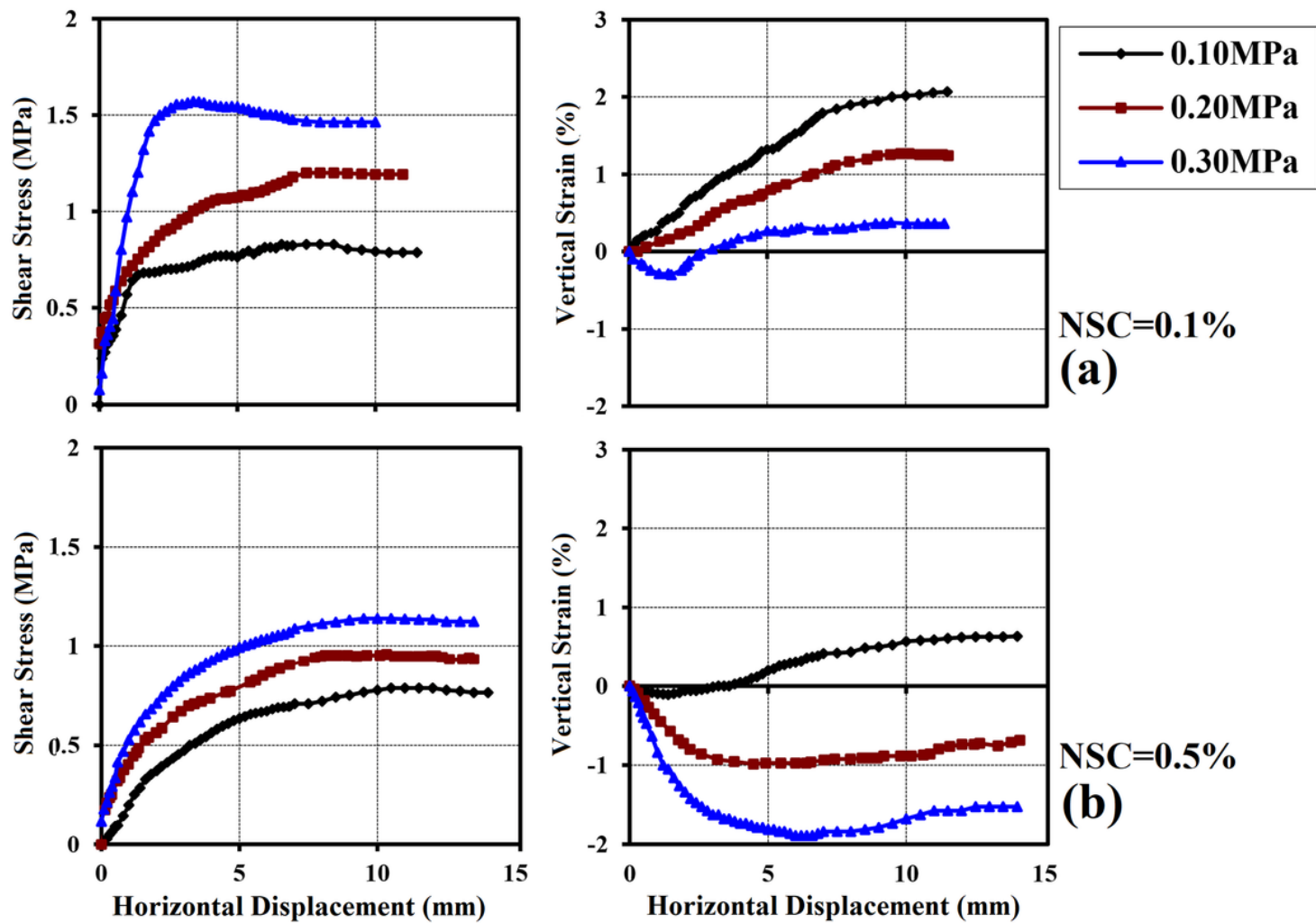
Figure 7

Shear stress-shear strain and vertical strain-shear strain curves of ceramic-fiber-reinforced specimens at a fiber length of 6 mm and nanosilica content of: (a) 0.1%, (b) 0.5%.
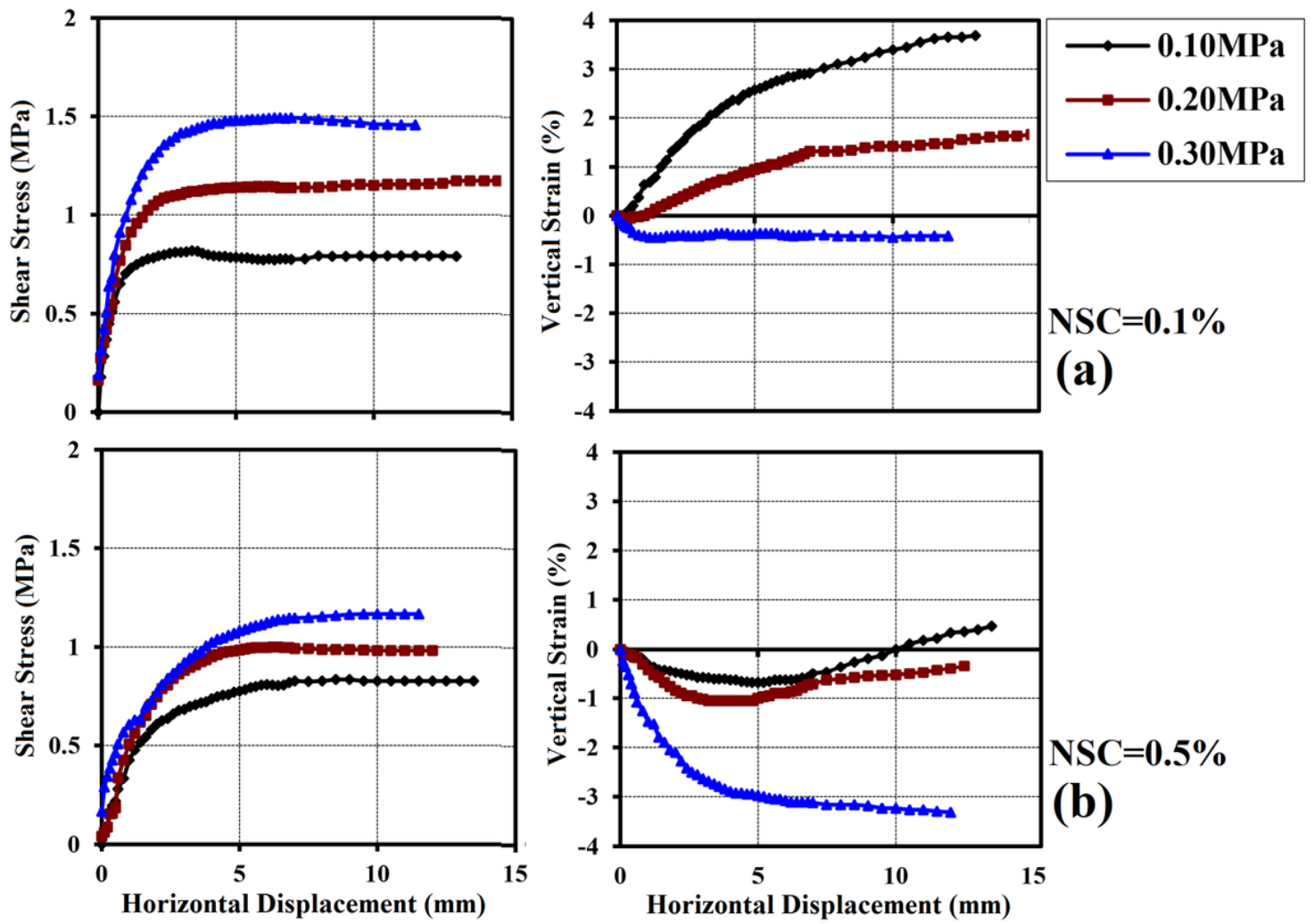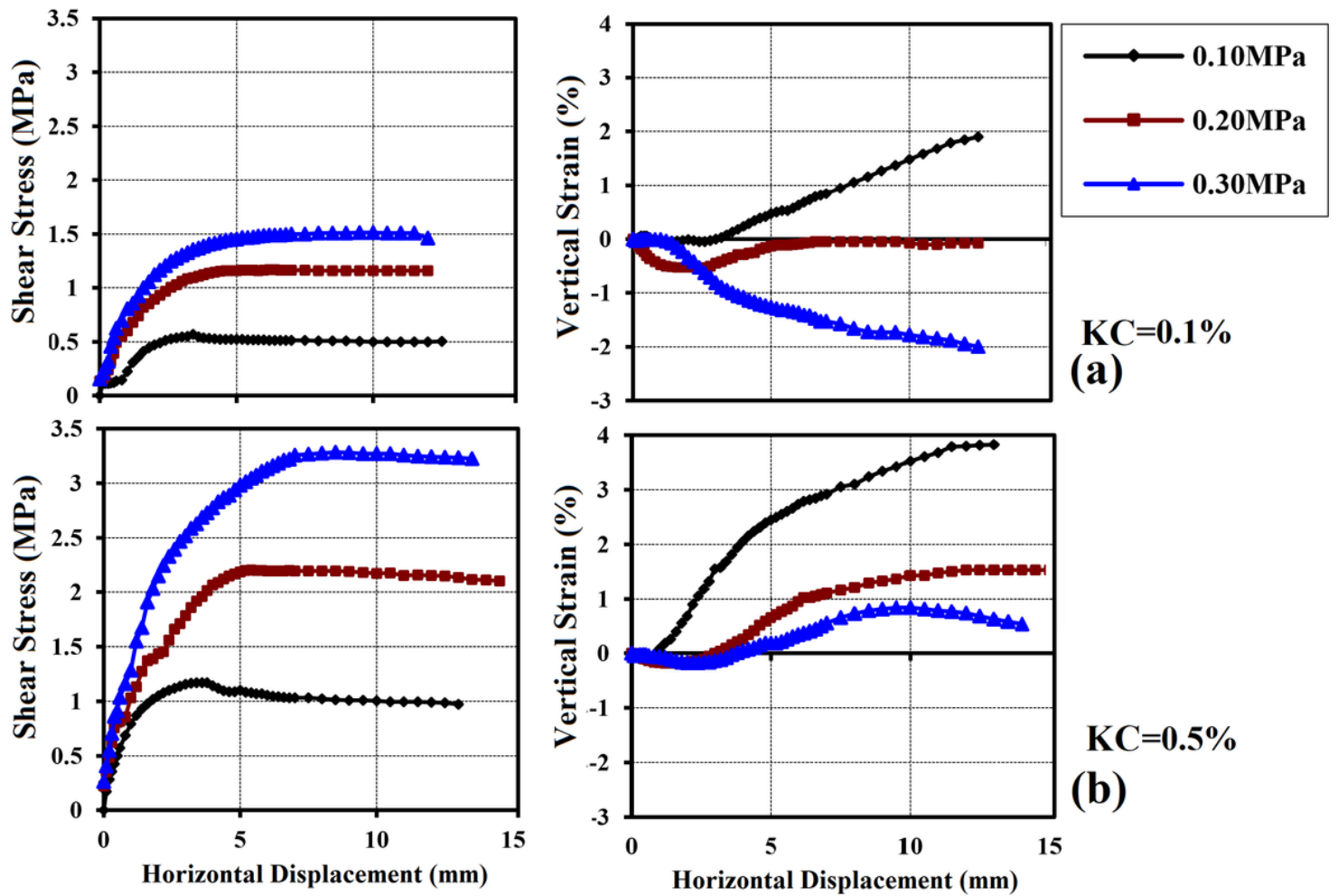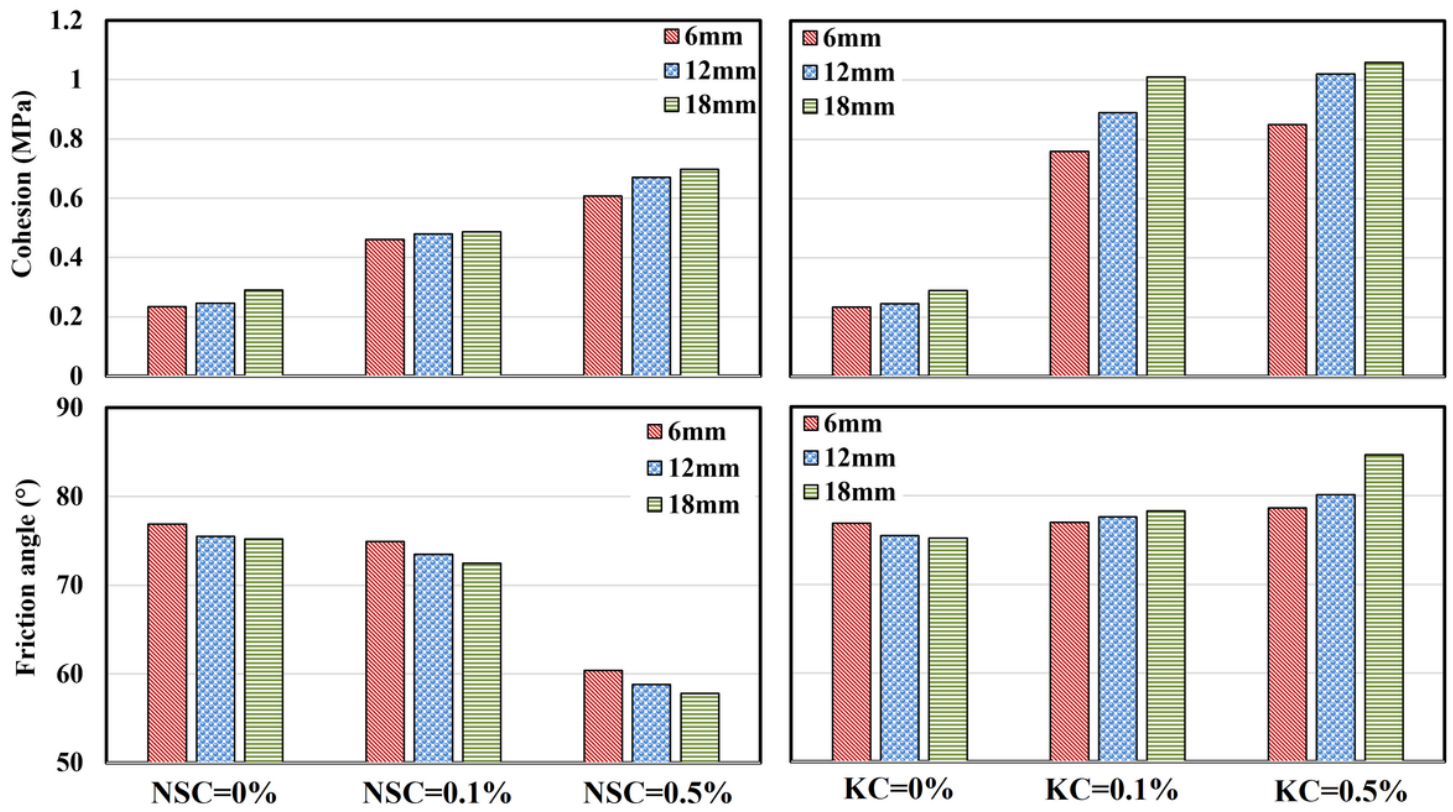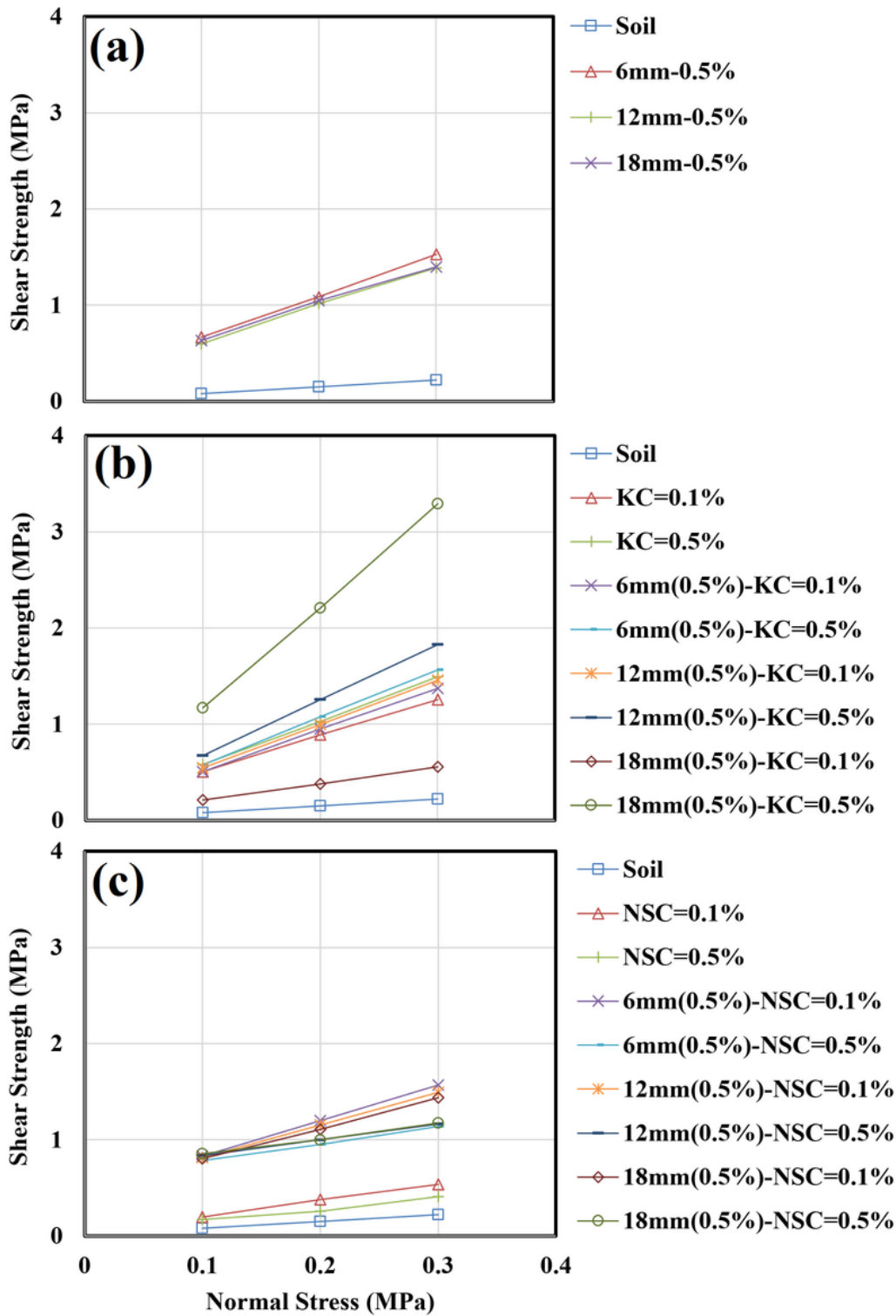
Figure 8

Shear stress-shear strain and vertical strain-shear strain curves of ceramic-fiber-reinforced specimens at a fiber length of 12 mm and nanosilica content of: (a) 0.1%, (b) 0.5%.

Figure 9

Shear stress-shear strain and vertical strain-shear strain curves of ceramic-fiber-reinforced specimens at a fiber length of 18 mm and nanosilica content of: (a) 0.1%, (b) 0.5%.

Figure 10

Shear stress-shear strain and vertical strain-shear strain curves of ceramic-fiber-reinforced specimens at a fiber length of 6 mm and kaolin content of: (a) 0.1%, (b) 0.5%.

Figure 11

Shear stress-shear strain and vertical strain-shear strain curves of ceramic-fiber-reinforced specimens at a fiber length of 12 mm and kaolin content of: (a) 0.1%, (b) 0.5%.

Figure 12

Shear stress-shear strain and vertical strain-shear strain curves of ceramic-fiber-reinforced specimens at a fiber length of 18 mm and kaolin content of: (a) 0.1%, (b) 0.5%.

Figure 13

Effect of fiber length, nanosilica, content, and kaolin content on the friction angle and cohesion of specimens.

Figure 14

Direct shear strength envelopes of specimens reinforced with: (a) ceramic fibers, (b) ceramic fibers and kaolin particles, (c) ceramic fibers and nanosilica particles.
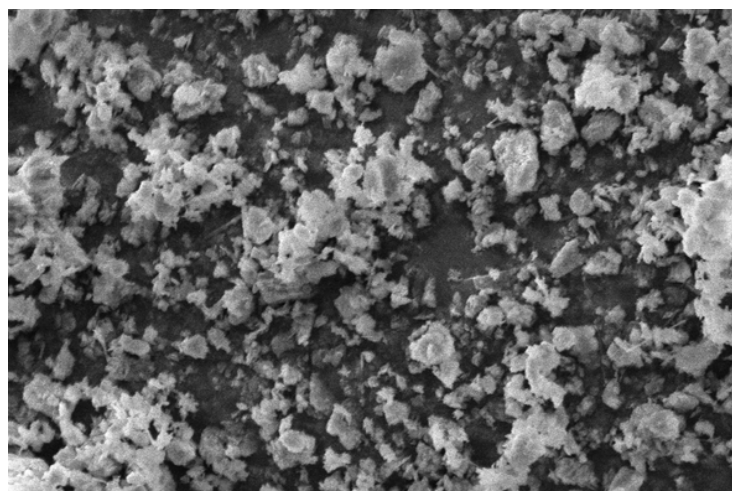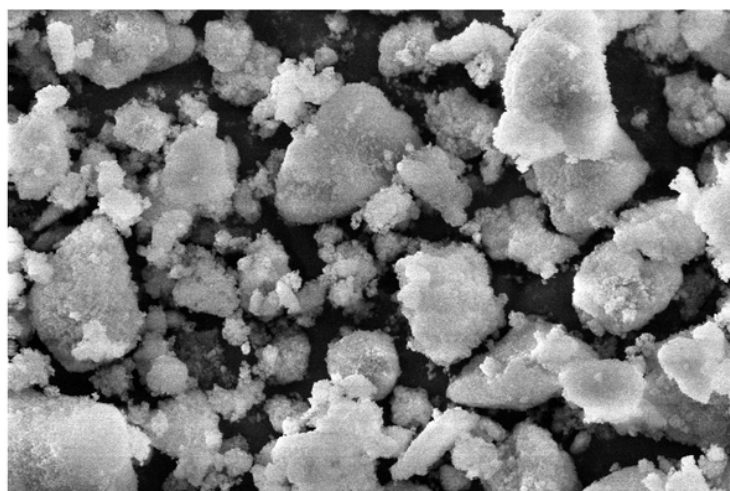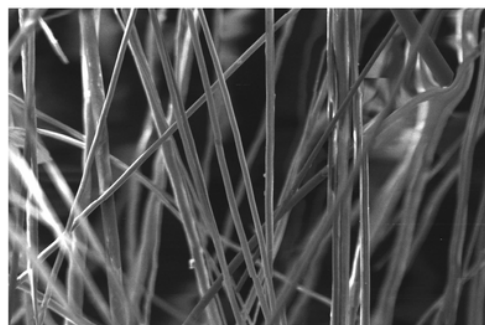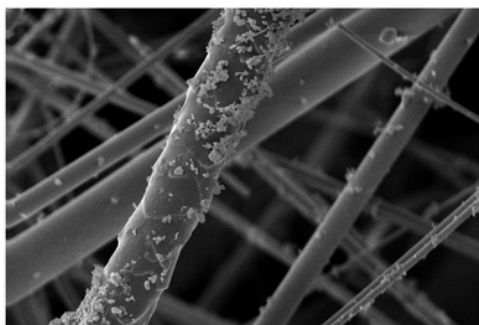
Figure 15

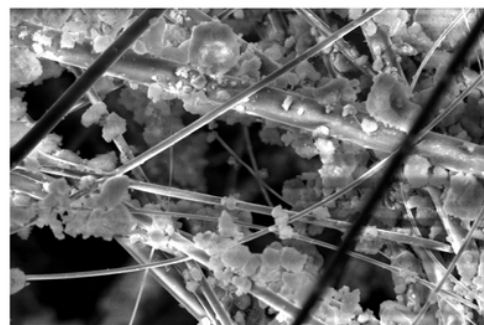SEM images of: (a) kaolin particles, (b) nanosilica particles.

Figure 16

SEM images of: (a) ceramic fibers, (b) ceramic fibers with kaolin-particle coating, (c) ceramic fibers with nanosilica-particle coating.